Phosphorus addition increased carbon partitioning to autotrophic respiration but not to biomass production in an experiment with Zea mays

Phosphorus addition increased carbon partitioning to autotrophic respiration but not to biomass production in an experiment with *Zea mays*

Running head:

P effects on plant C partitioning

ARNE VEN[1,2], MELANIE S VERLINDEN[2], ERIK FRANSEN[3], PÅL AXEL OLSSON[4], ERIK VERBRUGGEN[2], HÅKAN WALLANDER[4], SARA VICCA[2]

[1]*corresponding author*: *arne.ven@uantwerpen.be*

[2]*Research Centre of Excellence Plants and Ecosystems, Ecology in a time of change, University of Antwerp, BE-2610 Wilrijk, Belgium*

[3]*StatUa Center for Statistics, University of Antwerp, Belgium*

[4]*Department of Biology, Ecology Building, Lund University, S-223 62 Lund, Sweden*

ABSTRACT

Plant carbon (C) partitioning - the relative use of photosynthates for biomass production, respiration, and other plant functions - is a key but poorly understood ecosystem process. In an experiment with *Zea mays*, with or without arbuscular mycorrhizal fungi (AMF), we investigated the effect of phosphorus (P) fertilization and AMF on plant C partitioning. Based on earlier studies, we expected C partitioning to biomass production (i.e., biomass production efficiency; BPE) to increase with increasing P addition due to reduced C partitioning to AMF. However, although plant growth was clearly stimulated by P addition, BPE did not increase. Instead, C partitioning to autotrophic respiration increased. These results contrasted with our expectations and with a previous experiment in the same set-up where P addition increased BPE while no effect on autotropic respiration was found. The comparison of both experiments suggests a key role for AMF in explaining these contrasts. Whereas in the previous experiment substantial C partitioning to AMF reduced BPE under low P, in the current experiment, C partitioning to AMF was too low to directly influence BPE. Our results illustrate the complex influence of nutrient availability and mycorrhizal symbiosis on plant C partitioning.

KEY WORDS

arbuscular mycorrhizal fungi, autotrophic respiration, biomass production efficiency, carbon allocation, carbon balance, carbon partitioning, carbon use efficiency, phosphorus

INTRODUCTION

Plants take up carbon (C) from the atmosphere through photosynthesis (gross primary production, GPP). They allocate this C either to various organs and convert it into plant biomass production, export it to the rhizosphere (e.g. through symbiosis with mycorrhizal fungi) or use it to meet their energy requirements (Churchland *et al.*, 2013; Vicca *et al.*, 2012). This partitioning of assimilated C among functions determines the C residence time in the ecosystem and ultimately reflects the ecosystem C sink strength. It is a key ecosystem process that affects terrestrial biogeochemistry, through influences on litter quality and decomposition rates, C sequestration, and plant–atmosphere gas exchange (Cropper & Gholz, 1994; Friedlingstein *et al.*, 1998; Bird & Torn, 2006).

Plant C partitioning can vary strongly (Litton *et al.*, 2007; Verlinden *et al.*, 2018). While in some ecosystems C partitioning to plant biomass is only about 30%, others use up to 70% of the photosynthates for biomass production (DeLucia *et al.*, 2007; Litton *et al.*, 2007; Vicca *et al.*, 2012; Raich *et al.*, 2014; Campioli *et al.*, 2015). It is not clear yet why this variation occurs, but evidence is growing that nutrient availability plays a key role (Vicca *et al.*, 2012; Buendía *et al.*, 2014; Collalti & Prentice, 2019).

Phosphorus (P) and nitrogen (N) are globally the most limiting nutrients for plant growth (Elser *et al.*, 2007; LeBauer & Treseder, 2008), and variation in their availability can strongly impact plant C partitioning. For example, annual plant growth is typically more responsive to variation in nutrient availability than photosynthesis resulting in enhanced ratio of total plant biomass production to photosynthesis (i.e. biomass production efficiency; BPE) with increasing nutrient availability (e.g. Vicca *et al.*, 2012; Verlinden *et al.*, 2018). And while partitioning to aboveground growth usually increases with increasing P and N availability, belowground C partitioning generally decreases (Ericsson, 1995; Lilleskov *et al.*, 2002; Treseder, 2004; Vicca *et al.*, 2012), as plants then need to invest less to acquire P (Ekblad *et al.*, 1995; Johnson, 2010).

While both N and P are important regulators of C partitioning, their influence remains poorly quantified (Treseder, 2004; Gill & Finzi, 2016; Verlinden *et al.*, 2018).

Plants respire a large fraction of their GPP, with autotrophic respiration relative to GPP (R_{aut}:GPP) typically around 0.5 (Collalti & Prentice, 2019). From a plant physiology perspective it is often argued that autotrophic respiration is a relatively constant fraction of GPP due to interdependencies of respiration and photosynthesis (Dewar *et al.*, 1998; Hoefnagel *et al.*, 1998; van Oijen *et al.*, 2010). Several studies have confirmed a relatively constant respiration-to-photosynthesis ratio across species and ecosystems (Reich *et al.*, 1998; Loveys *et al.*, 2003; Turnbull *et al.*, 2005), but deviations from this pattern have also been observed, especially when circumstances were more extreme (e.g. at high temperatures; Atkin *et al.*, 2007; Campbell *et al.*, 2007; Drake *et al.*, 2016). Although the influence of nutrient availability on C partitioning to R_{aut} is still poorly understood, the limited evidence available suggests no effect of nutrient availability on R_{aut}:GPP (Vicca *et al.*, 2012 and references therein; Verlinden *et al.*, 2018). However, generalizations about influences of nutrients on R_{aut}:GPP are often impeded primarily due to limited availability of accurate and mutually independent quantifications of both biomass production (BP) and R_{aut} (Collalti & Prentice, 2019).

The majority of vascular plants live in symbiosis with AMF, where plants provide C by transferring carbohydrates via roots, while AMF supply their host with nutrients, especially P (Smith & Read, 2008; Brundrett, 2009; Johnson, 2010). One of the more widely tested hypotheses within the field of mycorrhizal ecology is that mycorrhizal fungi grow better and are more abundant when nutrient availability is low (Mosse & Phillips, 1971); when N or P availability rises, plants invest less C in nutrient acquiring mechanisms, which generally reduces mycorrhizal abundance (Treseder, 2004). This response is not universal, however, and N or P addition can even increase AMF growth under (strongly) nutrient-limited conditions (Treseder & Allen, 2002; Raven *et al.*, 2018). Given their central role in plant nutrient

93 acquisition, also plant C partitioning is expected to be influenced by AMF. For example, a
94 lower C cost for mycorrhizal symbiosis with increasing nutrient availability has been suggested
95 as the underlying mechanism explaining the typical increase of BPE with increasing nutrient
96 availability (Jakobsen & Rosendahl, 1990; Vicca *et al.*, 2012; Verlinden *et al.*, 2018). However,
97 this remains to be verified empirically.
98 We set up a fertilization experiment with a soil originally limiting in P but not in N to
99 investigate the effect of different levels of P fertilization on plant C partitioning, including BPE
100 and R_{aut}:GPP. We also compared mesocosms with and without AMF. The main hypothesis was
101 that BPE increases with increasing P fertilization due to reduced investment in AMF symbiosis,
102 while R_{aut}:GPP was expected to be relatively constant among treatments. A similar experiment
103 was conducted one year earlier, using the same set-up, but with N, P and N + P fertilization
104 instead of a P gradient (Verlinden *et al.*, 2018). This experiment showed that the growth of
105 maize in these soils was strongly limited by P availability, while N was ample as N addition
106 did not affect plant growth (Verlinden *et al.*, 2018). In the current study, we therefore opted for
107 a P gradient instead of an NxP experiment; gradient studies are also especially useful for
108 establishing response functions that help to better constrain vegetation models (Vicca *et al.*,
109 2018). We also compare both experiments to gain better insight into plant C partitioning and
110 the role of AMF.

MATERIALS AND METHODS

Experimental set-up

The set-up consisted of 30 insulated mesocosms (1 m × 1.2 m × 0.6 m high). The set-up and soil mixture were the same as in Verlinden *et al.* (2018). For more information, see Appendix S1. The soil in each mesocosm from the previous experiment (Verlinden *et al.*, 2018) could be used to start the current experiment, since the $\delta^{13}C$ ratio of soil organic matter had hardly changed (<1‰ difference between both experiments; Table S1). After the previous experiment, soil was homogenized within each AMF-nutrient combination two months before its start. Lime was added again to increase the pH on average to 6.19 (± 0.34). The soil of the same mesocosms as the previous experiment was pasteurized again by heating it for four hours at 80 °C to create ten AMF-free mesocosms. While N was sufficiently present and N fertilization in all mesocosms ensured no N limitations (see Verlinden *et al.*, 2018), we created a P-gradient by adding 2.5, 5, 10 or 20 kg P ha^{-1} (triple superphosphate; Janssens-Smeets®) to soil of 20 mesocosms containing unpasteurized soil (further referred to as P1, P2, P3 and P4 treatments, respectively; 5 replicates per treatment). The 10 pasteurized mesocosms received either the same amount of P as the P1 (P1_noAMF) or the P4 (P4_noAMF) treatments (also 5 replicates per treatment). Fourteen seedlings of *Zea mays* L. (a C_4-plant, variety 'Tom Thumb') per mesocosm were planted on the 21th of June 2017 after their roots were submerged in spore-based inoculum of the AMF *Rhizophagus irregularis* (Symplanta®). Mesh bags, often used to study AMF (see e.g. Ven *et al.*, 2020) because they exclude ingrowth of roots but are permeable for fungal hyphae (30 µm mesh, size 13 cm × 3 cm × 2 cm, average soil density 1.497 g cm^{-3}), filled with C free white river sand (heated for 5 hours at 550 °C to remove any remains of organic matter) were buried vertically into the top soil of each mesocosm one week before planting. One mesh bag per mesocosms was harvested at the end of the experiment, which was 10 weeks after planting.

136 ***Measurements***

137 *Environmental variables*

138 In each mesocosm, soil water content was continuously measured using a reflectometer
139 (CS616, Campbell Scientific, Logan, Utah, USA). To avoid any water stress, we ensured that
140 soil water content (SWC) was always between 6% and 12%. Air temperature was logged
141 simultaneously from a centralized air thermometer in the greenhouse. Two soil temperature
142 sensors (NTC-WH probe, Carel Industries, Manheim, USA) were installed in each mesocosm;
143 soil temperature (°C) at 5 cm depth was logged every 15 minutes for each mesocosm.
144 Photosynthetic photon flux density (PPFD) was continuously logged from PPFD sensors (JYP
145 1000, SDEC, Reignac-sur-Indre, France).

146 *CO_2 flux measurements*

147 An overview of the mesocosm measurements and their calculations to estimate C assimilation
148 and partitioning can be found in Fig. 1. Mesocosm photosynthesis and respiration were
149 quantified by chamber measurements of CO_2 fluxes, for which two cuvettes (one of 0.5 m
150 height and one of 1.5 m height) were cross-calibrated at the start of the experiment (Fig. S1).
151 During the experiment, CO_2-efflux increased and was always lower than 1.8 µmol CO_2 m^{-2} s^{-1}
152 when the 0.5 m high cuvette was used while 1.85 µmol CO_2 m^{-2} s^{-1} was the lowest CO_2 flux
153 measured using the 1.5 m high cuvette. These measurements were conducted ten times during
154 the season (i.e. every week) for the inoculated mesocosms, and seven times during the season
155 for the pasteurized mesocosms. Depending on plant height, one of the cuvettes was coupled to
156 an EGM-4 infrared gas analyzer (PP Systems, Hitchin, UK) and used to cover the entire
157 mesocosm to measure the CO_2 flux, operating as a dynamic closed system (De Boeck *et al.*,
158 2007; Vicca *et al.*, 2007; Verlinden *et al.*, 2018). Net ecosystem (mesocosm) exchange (NEE)
159 of CO_2 was estimated from three to six measurements of 200 seconds per mesocosm at various
160 light intensities (as in e.g. Vicca *et al.*, 2007 and Verlinden *et al.*, 2018) between 0 and 1300

161 μmol m^{-2} s^{-1} of PPFD using cloths of different transparency covering the mesocosm,
162 attenuating incoming light. The CO_2 effluxes in a fully darkened cuvette represented total
163 mesocosm CO_2 efflux (R_{eco}). GPP was then estimated by summing NEE and R_{eco}.
164 Soil CO_2 efflux was measured weekly on a shallow inox collar (8 cm high, 7.5 cm ∅) which
165 had been installed at 4 cm depth in each mesocosm prior to planting. Measurements were made
166 using a custom-built cuvette (7.5 cm ∅, 16 cm height) coupled to an EGM-4 infrared gas
167 analyser (PP Systems, Hitchin, UK) operating as a dynamic closed system. We measured the
168 increase in soil CO_2 concentration on this shallow collar (R_{soil}) during 120 seconds.
169 Additional to these measurements, from the fourth week until the end of the experiment, soil
170 CO_2 efflux and its $\delta^{13}C$ signal were measured weekly (inoculated mesocosms) or every two
171 weeks (pasteurized mesocosms) on the shallow collar and on an additional mesocosm-deep
172 collar (60 cm high, 7.5 cm ∅). This collar covered the entire soil depth and thus prevented
173 roots and fungi from growing in. Soil moisture inside these collars was measured every two
174 weeks, and kept at field capacity, similar to the surrounding soil. The CO_2 efflux and the $\delta^{13}C$
175 signal were measured using a custom-built cuvette (7.5 cm Ø, 16 cm height) and a G2131-i
176 CRDS isotopic-CO_2 gas analyser (Picarro Inc., Santa Clara, CA, USA) operating as a dynamic
177 closed system. We targeted an increase of the CO_2 concentration inside the cuvette of at least
178 100 ppm which required between 5 and 15 minutes. Given the naturally occurring difference
179 in $\delta^{13}C$ between the C_4 plants and the C_3 soil (in this experiment on average -12.25 in roots and
180 -25.6 in soil; Table S1), these $\delta^{13}C$ flux measurements allowed distinguishing plant-derived C
181 from C originating from the soil organic matter (see eq. S3 in Appendix S4, where we also
182 refer to Table S2 and Fig. S2).
183 As a complement to the mesocosm-scale chamber measurements, respiration and
184 photosynthesis were measured also at leaf scale (Table S3). A portable LI-COR gas exchange
185 system LI-6400 (Biosciences, Lincoln, NE, USA) was used, operating as an open system. Net

186 CO_2 assimilation rate was measured at 26 °C and photosynthetic photon flux densities (PPFD)
187 of 1200 µmol m^{-2} s^{-1} (considered as maximal assimilation rate; A_{max}) and 0 µmol m^{-2} s^{-1} (net
188 assimilation at zero light, considered as 'respiration in the dark' (R_{dark})). The ratio R_{dark}:A_{max}
189 served as an indication of the fraction of photosynthates used in plant respiration.
190 For GPP, R_{eco} and R_{soil} we followed the same protocol as Verlinden *et al*. (2018); see also
191 Halbritter *et al*. (2019). For each treatment, we fitted light response curves for GPP and
192 temperature response curves for R_{eco} and R_{soil}. These were upscaled to the entire growing
193 season to obtain a mean seasonal value and standard error (SE) for GPP ($\sum$GPP), R_{eco} ($\sum R_{eco}$)
194 and R_{soil} ($\sum R_{soil}$) (we refer to Appendix S2, Appendix S3, and Tables S4, S5, S6, S7, S8 and
195 S9 for more details regarding these calculations). The mean seasonal aboveground respiration
196 ($\sum R_{above}$) was estimated as $\sum R_{eco}$ - $\sum R_{soil}$. SE of the mean was calculated by error propagation.
197 As previously described in Ven *et al.* (2019), we calculated rhizosphere respiration (R_{rhizo})
198 using the Picarro CO_2 effluxes and associated $\delta^{13}C$ from the two collars installed in each
199 mesocosm, to estimate total R_{rhizo} ($\sum R_{rhizo}$) over the entire growing season (see Appendix S4).
200 SE of $\sum R_{rhizo}$ was calculated by error propagation.
201 *Plant biomass measurements and plant tissue P concentration*
202 On 31 August 2017, when plant growth had stopped and corn cobs had ripened, aboveground
203 and belowground plant biomass were harvested for all treatments, except for P1_noAMF where
204 they had been harvested 9 days earlier because plants had died prematurely. All aboveground
205 plant biomass was harvested in each mesocosm; belowground plant biomass was sampled
206 taking six cores (7 cm ∅, entire soil depth). To approach a spatially representative estimate of
207 belowground plant biomass production, two cores were collected on a stubble and the
208 remainder at variable distances between the stubbles. Soil cores were sieved and roots were
209 washed manually. Biomass was oven dried for 72 h at 70 °C. Subsamples were ground for
210 further analyses.

For each mesocosm, the $\delta^{13}C$ of the roots was determined on a 2 mg subsample (Elemental Analysis – Isotope Ratio Mass Spectrometry (EA-IRMS) using a CE Instrument EA 1110 elemental analyser, coupled to a Finnigan MAT DeltaPlus IRMS with a Finnigan MAT ConFlo II Interface). The C concentration of different plant parts (roots, leaves, stems, cobs) was determined using an elemental analyser (Flash 2000, Thermo Fisher Scientific, Germany). P concentration (g P g^{-1} dry biomass) of each plant part was analysed after acid destruction using H_2SO_4, salicylic acid, H_2O_2 and selenium (Walinga *et al.*, 1989). For each mesocosm, total plant biomass production (BP_{tot}) and P contents (P_{tot}) were calculated multiplying the biomass with C and P concentrations of the different plant parts. For each mesocosm, aboveground plant biomass production (BP_{above}) and belowground plant biomass production (BP_{root}) were calculated from the biomass and plant part-specific C concentrations. For each mesocosm, BPE was estimated as the fraction of BP_{tot} to the average $\sum$GPP of its treatment.

C budget imbalance

To assess the robustness of our C partitioning estimates, we verified for each treatment the closure of the C balance, with $\sum$GPP equalling the total C input, and the sum of $\sum R_{aut}$ and BP_{tot} (averaged per treatment) equalling total C output:

$$\text{C budget imbalance} = \text{total C input} - \text{total C output} = \sum GPP - (\sum R_{aut} + BP_{tot}) \quad \text{(eq. 1)}$$

The relative C budget imbalance was calculated as:

$$\text{relative C budget imbalance} = \text{C budget imbalance} : \sum GPP \quad \text{(eq. 2)}$$

SE was calculated using error propagation.

In our experiment, we did not explicitly include C partitioning to root exudation and mycorrhizal biomass. However, these C fluxes are indirectly included in $\sum R_{aut}$, since we assume turnover of both is fast (Olsson & Johnson, 2005; Phillips *et al.*, 2011; Ekblad *et al.*, 2016), and both are thus largely captured by R_{rhizo} (as part of R_{aut}).

Mycorrhizal colonization

Mycorrhizal root colonization and hyphal length followed the procedure described by Ven *et al.* (2020). Mycorrhizal root colonization was verified in August by sampling roots from four plants per mesocosm. Per plant, 20 cm of one lateral root containing root hair, was excavated, cut and stored for maximal two days at 5 °C. These roots were cleared and stained using a non-vital staining technique (as described by Vierheilig *et al.*, 2005), using a 5% KOH-solution and a Sheaffer Black Ink solution (10% ink in a 10% acetic acid solution). Mycorrhizal root colonization was quantified by counting arbuscules, vesicles and hyphae applying the gridline intersection method (Giovannetti and Mosse 1980, Brundrett *et al.*, 1996, Vierheilig *et al.*, 2005).

Hyphae were extracted from 4 g mesh bag sand following the approach of Rillig *et al.* (1999). See Appendix S5 for details. Hyphal intersects were counted at 400 × magnification at 25 locations on the filter using a grid inside the microscope ocular. Hyphal length density (HLD) was calculated using equation 3 (Rillig *et al.*, 1999; Tennant, 1975):

$$HLD = (\pi \cdot N \cdot A \cdot D)\,(H \cdot W)^{-1}, \quad \text{(eq. 3)}$$

with HLD = hyphal length density (mm hyphae g^{-1} soil), N = number of intersects where AMF hyphae were present, A = area of filter (mm^2) that was examined, D = dilution factor, H = total length of raster lines projected on filter (mm), and W = soil weight (g).

Statistical analysis

Statistical analyses were performed in R (RStudio Team, 2016). We had two types of variables: 1) 'Data_type1', was comprised of variables that were estimated for each mesocosm separately: BP_{root}, BP_{above}, BP_{tot}, R_{dark}:A_{max}, mycorrhizal colonization in roots, and HLD. Also BP_{root}:∑GPP, BP_{above}:∑GPP, and BPE (i.e. BP_{tot}:∑GPP) were calculated for each mesocosm separately (but using the treatment ∑GPP value; see data_type2); 2) 'Data_type2', were variables with only one value per treatment. These combined data from all mesocosms of a treatment to enable robust fitting of temperature or light response curves : ∑GPP, $\sum R_{rhizo}$,

261 $\sum R_{above}$, $\sum R_{aut}$, $\sum R_{rhizo}$:$\sum$GPP, $\sum R_{above}$:$\sum$GPP, $\sum R_{aut}$:$\sum$GPP. Given that $\sum$GPP and $\sum R_{aut}$ were
262 data_type2, also the C budget imbalance and relative C budget imbalance were data_type2.
263 BP_{tot} was averaged per treatment for these calculations (i.e., converted from data_type1 to
264 data_type2; see eq. 1). Data analyses differed between both types in that data_type2 represented
265 only a summary value with a standard error, calculated using error propagation. Therefore,
266 variables belonging to data_type2 were analysed with a weight variable, inversely proportional
267 to the standard error. This approach does not allow calculation of the correlation coefficient
268 (R^2), which is thus not presented for data_type2.
269 For each treatment a 95% confidence interval was calculated as 1.96 × SE to check if the C
270 budget imbalance differed from zero. A linear model was fitted to test the correlation between
271 P fertilization level (2.5, 5, 10 and 20 kg P ha^{-1}) and data_type1 in inoculated mesocosms. This
272 linear model was also fitted for data_type2.
273 Additionally, a one-way analysis of variance (ANOVA) was carried out for inoculated
274 mesocosms to test if data_type1 differed between 2.5, 5, 10 and 20 kg ha^{-1} as four independent
275 treatments: 'P1, 'P2', 'P3' and 'P4' respectively. Pairwise differences between these treatments
276 were estimated using a posthoc analysis with Tukey's Honest Significant Difference
277 (TukeyHSD) method for multiple hypothesis testing. For $\sum$GPP, which in inoculated
278 mesocosms could be estimated for each of the nine measuring periods separately, pairwise
279 differences between the four treatments were calculated using R-package 'multcomp' and its
280 Simultaneous Tests for General Linear Hypotheses (SGLH) with the 'Tukey Contrasts'
281 method, with measuring period as independent variable and the inverse of the SE of each
282 treatment in every nine measurement periods added as weight. In other data_type2 datasets,
283 where only one average value per treatment over all measurement periods could be calculated,
284 significance of differences between two treatments was tested by directly filling in the test

statistic of the t-test, with differences between the two means in the numerator, and the common standard error (calculated by error propagation) in the denominator.

A t-test using only the pasteurized 'P4_noAMF' and inoculated soil 'P4' treatment was applied to test the pasteurization effect on data_type1 datasets. For ∑GPP, this pasteurization effect was calculated using R-package 'multcomp' and its SGLH with the 'Dunnett Contrasts' method, with measuring period as independent variable and weighting the observations by the inverse of the standard error. In the other data_type2 datasets, the significance of the pasteurization effect was estimated as described above, directly filling out the difference between P4 and P4_noAMF in the numerator of the test statistic for the t-test, and divided by their common SE (calculated using error propagation).

RESULTS

For all treatments, the C budget imbalance was relatively small, and for treatments P1, P2, P3 and P4_noAMF, this was not significantly different from zero (Table 1). Only in treatment P4, the 'C budget imbalance' was significantly negative (Table 1). Fertilization or pasteurization did not significantly affect the C budget imbalance (Table 1). The relative C budget imbalance (i.e., relative to ∑GPP) varied between -0.06 and 0.01 for all treatments and did not significantly differ among treatments (Table 2). Pasteurization had no effect on this relative C budget imbalance (Table 2).

∑GPP, $\sum R_{rhizo}$, $\sum R_{above}$, $\sum R_{aut}$ (the sum of $\sum R_{rhizo}$ and $\sum R_{above}$), BP_{root}, BP_{above} and BP_{tot} (the sum of BP_{root} and BP_{above}) all increased or tended to increase with increasing P fertilization (Table 1), while pasteurization (P4 vs. P4_noAMF) significantly decreased all these estimates of plant growth and activity (Table 1). Both $\sum R_{above}$:∑GPP and R_{dark}:A_{max} increased with increasing P fertilization ($p \leq 0.06$). $\sum R_{rhizo}$:∑GPP, on the other hand, was not affected by P fertilization (Table 2). $\sum R_{aut}$:∑GPP did significantly increase with increasing P fertilization

(Fig. 2). Pasteurization had a significantly positive effect on $\sum R_{above}$:$\sum$GPP, but a significantly negative effect on $\sum R_{rhizo}$:$\sum$GPP, and no significant effect on R_{dark}:A_{max} or $\sum R_{aut}$:$\sum$GPP (Table 2, Fig. 2).

The relationships for BP_{above}:$\sum$GPP and BP_{root}:$\sum$GPP versus P fertilization were not statistically significant. Nonetheless, BP_{root}:$\sum$GPP was twice as large in P1 and P2 as compared to P3 and P4, with a significant difference between P1 and P2 vs P3 and P4 (Table 2). Also BPE tended to decrease with P fertilization and ANOVA showed a significant difference between treatments: both P4 and P3 < P2 (both $p = 0.01$). Pasteurization did not affect BP_{root}:$\sum$GPP, BP_{above}:$\sum$GPP or BPE (Table 2, Fig. 2).

Mycorrhizal colonization in roots significantly increased with P fertilization when expressed as % of roots colonized by arbuscules (on average ± 10% in P1, P2 and P3 vs. 22% in P4), had a trend towards a significant increase with P fertilization when expressed as % of roots colonized by hyphae (on average ± 35 to 60%), and did not increase with P fertilization when expressed as % of roots colonized by vesicles (on average approx. 10 to 30 %; Table 3). Despite substantial root colonization (Table 3), HLD in soil was low (Fig. 3; HLD 50 % lower than in Verlinden *et al.*, 2018). P fertilization significantly increased the hyphal length density (HLD), although this correlation was rather weak (after ln-transformation, Fig. 3A). In the pasteurized mesocosms, no mycorrhizal structures were found in roots or soil (Table 3, Fig. 3).

DISCUSSION

To verify the robustness of our estimation of C partitioning to R_{aut} and to plant growth, we confirmed the closure of the C balance; a closed C balance indicates robust estimation of partitioning. This was the case for all treatments except for P4, where the C budget imbalance indicated an underestimation of C input ($\sum$GPP) and/or overestimation of C outputs ($\sum R_{aut}$ and/or $\sum BP_{tot}$; see eq. 1). Importantly, the relative C budget imbalance was small for all

335 treatments (no more than 6% of assimilated C) and was not significantly affected by P
336 fertilization. We can thus assume that the observed fertilization effects on C partitioning were
337 not biased by the methodological challenge to close the C balance. In our calculations, we
338 further assume that C partitioning to root exudation and to AMF was largely captured by R_{rhizo},
339 because turnover of both is fast (Olsson & Johnson, 2005; Phillips *et al.*, 2011; Ekblad *et al.*,
340 2016). The pasteurized treatment, where the absence of AMF was expected to facilitate the C
341 balance-closure, allowed us to verify this assumption. The lack of a negative pasteurization
342 effect on the (relative) C budget imbalance of the P4 treatment confirms that C partitioning to
343 root exudation and mycorrhizal symbiosis was largely captured by R_{rhizo}.
344 Increasing P fertilization clearly increased $\sum GPP$, $\sum R_{aut}$ and BP, indicating that P availability
345 limited plant growth and activity in the lower P treatments. The largest increase was observed
346 for $\sum GPP$, indicating that $\sum GPP$ is more sensitive to changes in P availability than BP. This
347 contrasted with our expectation that plant growth would be more responsive to variation in
348 nutrient availability than photosynthesis (e.g. Vicca *et al.*, 2012; Verlinden *et al.*, 2018). The P
349 limitation was also reflected in the P-induced decrease of BP_{root}:$\sum GPP$, which was twice as
350 large in P1 and P2 as compared to P3 and P4. Increasing nutrient availability often reduces the
351 need of plants to invest C belowground for acquiring nutrients, leaving more C for aboveground
352 growth (Lilleskov *et al.*, 2002; Treseder, 2004; Vicca *et al.*, 2012). Surprisingly, the reduction
353 in BP_{root}:$\sum GPP$ with P fertilization in our experiment was not associated with an increase in
354 BP_{above}:$\sum GPP$, and C partitioning to BP_{tot}, i.e. BPE, even tended to decrease with increasing P
355 fertilization. This contrasts with our hypothesis and with earlier research (e.g. Litton *et al.*,
356 2007; Vicca *et al.*, 2012; Verlinden *et al.*, 2018). The tendency for a decrease instead of an
357 increase of BPE with increasing P fertilization implies that P fertilization either increased C
358 partitioning to plant respiration, increased C partitioning to symbionts and exudates, or a
359 combination of both.

C partitioning to autotrophic respiration ($\sum R_{aut}$:$\sum$GPP) indeed increased with increasing P fertilization. However, $\sum R_{aut}$ includes $\sum R_{rhizo}$ which at least partly captured symbionts and exudates in our calculations. Distinguishing above- versus belowground patterns provides further insights in the underlying processes. Both $\sum R_{above}$:$\sum$GPP and the leaf respiration-to-photosynthesis ratio (R_{dark}:A_{max}; see Table S3) increased with increasing P fertilization. This supports studies that indicated that the respiration-to-photosynthesis ratio may be less constant than previously assumed, especially under less favourable growth conditions (Atkin *et al.*, 2007; Campbell *et al.*, 2007; Drake *et al.*, 2016; Collalti & Prentice, 2019). In contrast to these aboveground patterns, $\sum R_{rhizo}$:$\sum$GPP was unaffected by P fertilization. We can thus conclude that the decreasing trend in BPE with increasing P fertilization was primarily linked to increased C partitioning to plant respiration, especially aboveground. Possibly, mass-specific leaf respiration increased with increasing P due to increased labile carbon following low sink demand (Mahmud *et al*., 2018). Such effect may be more likely to occur when AMF abundance is low (Valentine *et al*., 2001), as was the case in our experiment, but we do not have the data to verify whether sink limitation occurred in our experiment.

The relatively constant $\sum R_{rhizo}$:$\sum$GPP contrasted with the reduction of BP_{root}:$\sum$GPP with increasing P fertilization. Hence, the reduced C partitioning to root biomass production appeared to be counterbalanced by C partitioning to other belowground processes, such as mycorrhizal symbiosis, exudation and/or root respiration, as reflected also in the increase of $\sum R_{rhizo}$:BP_{root} with increasing P (Table S10). Although AMF abundance was low, root mycorrhizal colonization and HLD (a proxy for AMF biomass) increased with increasing P availability and the possibility for an increased contribution of AMF to $\sum R_{rhizo}$:GPP with increasing P fertilization is supported by the difference between inoculated and pasteurized mesocosms. Both $\sum R_{rhizo}$:$\sum$GPP and $\sum R_{rhizo}$:BP_{root} were smaller for the pasteurized treatment (Tables 2 and S10). On the other hand, we cannot exclude the possibility that C partitioning to

385 exudation and/or root respiration contributed to the increasing $\sum R_{rhizo}$:BP_{root} with increasing P.
386 Our data do not allow to further unravel the contribution of these processes; in future
387 experiments, measurements of specific root respiration can provide further insight into these
388 mechanisms.
389 The unexpected decreasing trend for BPE in response to P fertilization contrasted with the P-
390 induced increase of BPE observed in a similar experiment conducted one year earlier
391 (Verlinden *et al.*, 2018; Fig. 2). In this previous experiment, the same set-up, soil and plant
392 species were used, but fertilizer treatments differed (full factorial N×P experiment; see methods
393 and Verlinden *et al.*, 2018). Given that the mesocosms of P1 and P4 received comparable
394 amounts of P in both experiments, and N fertilization did not affect plant growth or C
395 partitioning in the previous experiment, the contrasting response of BPE to P fertilization is
396 unlikely due to differences in fertilizer treatments between both experiments. Even though
397 $\sum R_{aut}$:$\sum$GPP could only be estimated indirectly in the previous experiment (i.e., as the residual
398 C needed to close the C balance), also these patterns clearly differed between both experiments:
399 both $\sum R_{aut}$:$\sum$GPP and R_{dark}:A_{max} increased with P fertilization in the current experiment but
400 were relatively constant in the previous experiment. These differences between both
401 experiments emphasize a fundamental difference in the C partitioning process.
402 A remarkable difference between both experiments was the degree of AMF abundance in soil;
403 the amount of AMF was much lower in the current than in the previous experiment (e.g., HLD
404 in the current experiment was only about half the amount of the previous experiment; Fig. 3).
405 This may indicate a role for the AMF in explaining differences in C partitioning between both
406 experiments. This is further supported by the fact that the differences in BPE and $\sum R_{aut}$:$\sum$GPP
407 between both experiments were especially clear for their lowest fertilization level (Fig. 2),
408 where plants relied most on their symbionts for nutrient uptake. Combined, the two
409 experiments suggest that, when AMF abundance is high (exp. 1), plants growing on P poor soil

410 invest more of their photosynthates in these symbiotic partners, at the expense of C partitioning
411 to BP, hence resulting in an increase of BPE with increasing P fertilization. When AMF
412 abundance was low (exp. 2 and pasteurized treatment), possibly due to unfavourable soil
413 conditions, plant C partitioning responded very different, with no increase in C partitioning to
414 plant biomass, but increased partitioning to R_{aut}. Further experimental testing is needed to
415 verify this postulated role for AMF in plant C partitioning and to unravel the physiology behind
416 these differences.
417 A possible reason for the lower AMF growth in the current experiment is a reduction in soil
418 pH. Due to somewhat different liming treatments, the average soil pH declined from 6.19 to
419 5.43 during the current experiment (Table S11), while during the previous experiment soil pH
420 increased from 6.84 to 7.44 (Table S11). AMF typically thrive in high pH soils, (Marschner,
421 1998; Clark, 2002; van Aarle *et al*., 2002), and at high pH, P is increasingly locked up as
422 calcium phosphate, making plants more dependent on AMF for P acquisition (Larcher, 2003).
423 Despite their lower abundance in soil, AMF still seemed to have a positive effect on plant
424 performance in the current experiment. BP_{tot} and $\sum$GPP were about 50% higher in the
425 inoculated than in the pasteurized P4 mesocosms (P4 vs. P4_noAMF) and plants in pasteurized
426 P1 mesocosms (P1_noAMF) died prematurely while those in P1 survived the similarly low P
427 addition. Also the lower N:P ratio in leaves of AMF-colonized plants in comparison with leaves
428 of plants in pasteurized mesocosms indicate that plants were more P-stressed in the pasteurized
429 mesocosms (Table S12).
430 In summary, while previous research reported a decrease in BPE with decreasing nutrient
431 availability (Vicca *et al*., 2012), our experiment unveiled a more complex picture. The main
432 hypothesis that BPE increases with increasing P fertilization was refuted, and while R_{aut}:GPP
433 was expected to be relatively constant among treatments, we found an increase with increasing
434 P fertilization due to increased C partitioning to aboveground respiration. The difference

between pasteurized (no AMF) and AMF-inoculated treatments, together with the comparison with a previous experiment in a similar set-up, suggest a role for AMF in determining these C partitioning patterns; as suggested by Ven et al. (2019), AMF can reduce the C cost of P uptake, even when their abundance and hence their C use is low. Our results emphasize the need to take into account not only nutrient availability, but also mycorrhizal symbionts when studying and modelling C partitioning in terrestrial ecosystems.

ACKNOWLEDGEMENTS

This research was supported by the Research Foundation – Flanders (FWO) G0D5415N, the European Research Council grant ERC-SyG-610028 IMBALANCE-P, ClimMani COST Action (ES1308) and Methusalem funding of the Research Council UA. We acknowledge Fred Kockelbergh and Marc Wellens for technical support, and Bart Hellemans, Lin Leemans and Eddy De Smet for logistic support at the field site.

AUTHOR CONTRIBUTION

SV designed the research; AV and MV conducted the field- and lab work; AV drafted the paper; and AV, MV, EF, PAO, EV, HW and SV contributed to the interpretation of the results and to the writing of the paper, where EF and AV made statistical decisions and calculations.

CONFLICT OF ITEREST STATEMENT

The authors declare that there are no conflicts of interest regarding the publication of this paper.

REFERENCES

458 **Atkin O.K., Scheurwater I. & Pons T.L. (2007)** Respiration as a percentage of daily
459 photosynthesis in whole plants is homeostatic at moderate, but not high, growth temperatures.
460 *New Phytologist* **174,** 367-380.

461 **Balesdent J., MariottiA., Guillet B. (1987).** Natural ^{13}C abundance as a tracer for studies
462 of soil organic matter dynamics. *Soil Biology & Biochemistry* **19**, 25-30.

463 **Bird J.A. & Torn M.S. (2006)** Fine roots vs. Needles: A comparison of C-13 and N-15
464 dynamics in a ponderosa pine forest soil. *Biogeochemistry* **79**(3), 361-382.

465 **Brundrett M.N., Bougher B.D., Dell B., Grove T. & Malajczuk N. (1996)** Working with
466 Mycorrhizas in Forestry and Agriculture. *Australian Centre for International Agricultural*
467 *Research, Canberra, Australia.*

468 **Brundrett M.C. (2009)** Mycorrhizal associations and other means of nutrition of vascular
469 plants: understanding the global diversity of host plants by resolving conflicting information
470 and developing reliable means of diagnosis. *Plant and Soil* **320**(1-2), 37-77.

471 **Buendía C., Arens S., Hickler T., Higgins S.I., Porada P. & Kleidon A. (2014)** On the
472 potential vegetation feedbacks that enhance phosphorus availability – insights from a process-
473 based model linking geological and ecological timescales. *Biogeosciences* **11**, 3661-3683.

474 **Campbell C., Atkinson L., Zaragoza-Castells J., Lundmark M., Atkin O. & Hurry V.**
475 **(2007)** Acclimation of photosynthesis and respiration is asynchronous in response to changes
476 in temperature regardless of plant functional group. *New Phytologist* **176**, 375-389.

477 **Campioli M.S., Vicca S., Luyssaert S., Bilcke J., Ceschia E., Chapin lii F.S., … &**
478 **Janssens I.A. (2015).** Biomass production efficiency controlled by management in temperate
479 and boreal ecosystems. *Nature Geoscience* **8**, 843-846.

480 **Churchland C., Grayston S.J. & Bengtson P. (2013)** Spatial variability of soil fungal and
481 bacterial abundance: Consequences for carbon turnover along a transition from a forested to
482 clear-cut site. *Soil Biology & Biochemistry* **63**, 5-13.

Clark D.A. (2002) Are tropical forests an important carbon sink? Reanalysis of the long-term plot data. *Ecological Applications,* **12**(1), 3–7.

Collalti A. & Prentice I.C. (2019) Is NPP proportional to GPP? Waring's hypothesis twenty years on. *Tree Physiology* **in press**. DOI: 10.1093/treephys/tpz034

Cropper W.P.J. & Gholz H.L. (1994) Evaluating potential response mechanisms of a forest stand to fertilization and night temperatures: a case study of *Pinus elliottii*. *Ecological Bulletins* **43,** 154–160.

De Boeck H.J., Lemmens C.M., Vicca S., Van den Berge J., Van Dongen S., Janssens I.A., … & Nijs I. (2007) How do climate warming and species richness affect CO_2 fluxes in experimental grasslands? *New Phytologist* **175**, 512-522.

DeLucia E.H., Drake J.E., Thomas R.B. & Gonzalez-Meler M. (2007) Forest carbon use efficiency: is respiration a constant fraction of gross primary production? *Global Change Biology* **13**, 1157-1167.

Dewar R.C., Medlyn B.E. & McMurtrie R.E. (1998) A mechanistic analysis of light and carbon use efficiencies. *Plant, Cell and Environment* **21**, 573-588.

Drake J.E., Tjoelker M.G., Aspinwall M.J., Reich P.B., Barton C.V.M., Medlyn B.E. & Duursma R.A. (2016) Does physiological acclimation to climate warming stabilize the ratio of canopy respiration to photosynthesis? *New Phytologist* **211**(3), 850-683.

Elser J.J., Bracken M.E.S., Cleland E.E., Gruner D.S., Harpole W.S., Hillebrand H., … & Smith J.E. (2007) Global analysis of nitrogen and phosphorus limitation of primary producers in freshwater, marine, and terrestrial ecosystems. *Ecology Letters* **10**, 1135–1142.

Ekblad A., Wallander H., Carlsson R. & Huss-Danell K. (1995) Fungal biomass in roots and extrametrical mycelium in relation to macronutrients and plant biomass of ectomycorrhizal *Pinus sylvestris* and *Alnus incana*. *New Phytologist* **131**, 443-451.

Ekblad A., Mikusinska A., Agren G.I., Menichetti L., Wallander H., Vilgalys R., … & Eriksson U. (2016) Production and turnover of ectomycorrhizal extrametrical mycelial biomass and necromass under elevated CO2 and nitrogen fertilization. *New Phytologist* **211**(3), 874–885.

Ericsson, T. (1995) Growth and shoot-root ratio of seedlings in relation to nutrient availability. *Plant and Soil* **168**, 205-214.

Friedlingstein P., Joel G., Field C.B. & Fung I.Y. (1999) Toward an allocation scheme for global terrestrial carbon models. *Global Change Biology* **5**, 755–770.

Gill A.L. & Finzi A.C. (2016) Belowground carbon flux links biogeochemical cycles and resource-use efficiency at the global scale. *Ecology Letters* **19**(12), 1419-1428.

Giovannetti M. & Mosse B. (1980) Evaluation of techniques for measuring vesicular arbuscular mycorrhizal infections in roots. *New Phytologist* **84**(3), 489-500.

Halbritter A.H., De Boeck H., Eycott A.E., Reinsch S., Robinson D.A., Vicca S., … & Vandvik V. (2019) The handbook for standardised field and laboratory measurements in terrestrial climate-change experiments and observational studies (ClimEx). *Methods in Ecology & Evolution*. doi: https://doi.org/10.1111/2041-210X.13331

Hoefnagel M.H.N., Atkin O.K. & Wiskich J.T. (1998) Interdependence between chloroplasts and mitochondria in the light and the dark. *Biochimica et biophysica acta* **1366**, 235-255.

Jakobsen I. & Rosendahl L. (1990) Carbon Flow into Soil and External Hyphae from Roots of Mycorrhizal Cucumber Roots. *New Phytologist* **115**, 77-83.

Johnson N.C. (2010) Resource stoichiometry elucidates the structure and function of arbuscular mycorrhizas across scales. *New Phytologist* **185**(3), 631-647.

Larcher W. (2003) Physiological Plant Ecology (fourth edition). Berlin, Heidelberg, New York: Springer-Verlag.

LeBauer D.S. & Treseder K.K. (2008) Nitrogen limitation of net primary productivity in terrestrial ecosystems is globally distributed. *Ecology* **89**(2), 371-379.

Lilleskov E.A., Fahey T.J., Horton T.R. & Lovett G.M. (2002) Belowground ectomycorrhizal fungal community change over a nitrogen deposition gradient in Alaska. *Ecology* **83**, 104-115.

Litton C.M., Raich J.W. & Ryan M.G. (2007) Carbon allocation in forest ecosystems. *Global Change Biology* **13**(10), 2089–2109.

Loveys B.R., Atkinson L.J., Sherlock D.J., Roberts R.L., Fitter A.H. & Atkin O.K. (2003) Thermal acclimation of leaf and root respiration: an investigation comparing inherently fast- and slow-growing plant species. *Global Change Biology* **9**, 895-910.

Mahmud K., Medlyn B.E., Duursma R.A., Campany C. & De Kauwe M.G. (2018) Inferring the effects of sink strength on plant carbon balance processes from experimental measurements. *Biogeosciences*, **15**, 4003-4018.

Marschener H. (1998) Role of root growth, arbuscular mycorrhiza, and root exudates for the efficiency in nutrient acquisition. *Field Crops Research,* **56**(1-2), 203–207.

Mosse B. & Phillips J.M. (1971) The influence of phosphate and other nutrients on the development of vesicular-arbuscular mycorrhiza in culture. *Microbiology* **69**, 157-166.

Olsson P.A. & Johnson N.C. (2005) Tracking carbon from the atmosphere to the rhizosphere. *Ecology Letters* **8**(12), 1264–1270.

Phillips R.P., Finzi A.C. & Bernhardt E.S. (2011) Enhanced root exudation induces microbial feedbacks to N cycling in a pine forest under long-term CO_2 fumigation. *Ecology Letters* **14**, 1887-1894.

Raich J.W., Lambers H. & Oliver D.J. (2014) Respiration in Terrestrial Ecosystems. In: Holland HD, Turekian KK, eds. *Treatise on Geochemistry*, Second Edition, vol. 10. Elsevier, Oxford, UK, 613-649.

Raven J.A., Lambers H., Smith S.E. & Westoby M. (2018) Costs of acquiring phosphorus by vascular land plants: patterns and implications for plant coexistence. *New Phytologist* **217**(4), 1420–1427.

Reich P.B., Walters M.B., Ellsworth D.S., Vose J.M., Volin J.C., Gresham C. & Bowman W.D. (1998) Relationships of leaf dark respiration to leaf nitrogen, specific leaf area and leaf life-span: a test across biomes and functional groups. *Oecologia* **114**, 471-482.

Rillig M.C., Field C.B. & Allen M.F. (1999) Soil biota responses to long-term atmospheric CO2 enrichment in two California annual grasslands. *Oecologia* **119**(4), 572–577.

RStudio Team (2016) RStudio: Integrated Development for R. RStudio, Inc., Boston, MA URL http://www.rstudio.com/.

Smith S.E. & Read D.J. (2008) *Mycorrhizal symbiosis*. London, UK: Academic Press and Elsevier.

Tennant D. (1975) A test of a modified line intersect method of estimating root length. *The Journal of Ecology* **63**(3), 995–1001.

Treseder K.K. & Allen M.F. (2002) Direct nitrogen and phosphorus limitation of arbuscular mycorrhizal fungi: a model and field test. *New Phytologist* **155**(3), 507-515.

Treseder K.K. (2004) A meta-analysis of mycorrhizal responses to nitrogen, phosphorus, and atmospheric CO_2 in field studies. *New Phytologist* **164**, 347-355.

Turnbull M.H., Tissue D.T., Griffin K.L., Richardson S.J., Peltzer D.A. & Whitehead D. (2005) Respiration characteristics in temperate rainforest tree species differ along a long-term soil-development chronosequence. *Oecologia* **143**, 271-279.

Valentine A.J., Osborne B.A. & Mitchell D.T. (2001) Interactions between phosphorus supply and total nutrient availability on mycorrhizal colonization, growth and photosynthesis of cucumber. *Scientia Horticulturae* **88(3)**, 177-189.

581 **van Aarle I.M., Olsson P.A. & Soderstrom B. (2002)** Arbuscular mycorrhizal fungi
582 respond to the substrate pH of their extraradical mycelium by altered growth and root
583 colonization. *New Phytologist* **155**(1), 173–182.
584 **van Oijen M., Schapendonk A. & Höglind M. (2010)** On the relative magnitudes of
585 photosynthesis, respiration, growth and carbon storage in vegetation. *Annals of Botany* **105**,
586 793-797.
587 **Ven A., Verlinden M.S., Verbruggen E. & Vicca S. (2019)** Experimental evidence that
588 phosphorus fertilization and arbuscular mycorrhizal symbiosis can reduce the carbon
589 cost of phosphorus uptake. *Functional Ecology*. doi: 10.1111/1365-2435.13452
590 **Ven A., Verbruggen E., Verlinden M.S., Olsson P.A., Wallander H. & Vicca S. (2020)**
591 Mesh bags underestimated arbuscular mycorrhizal abundance but captured fertilization
592 effects in a mesocosm experiment. *Plant & Soil*. doi: 10.1007/s11104-019-04368-4
593 **Verlinden M.S., Ven A., Verbruggen E., Janssens I.A., Wallander H. & Vicca S. (2018)**
594 Favorable effect of mycorrhizae on biomass production efficiency exceeds their carbon costs
595 in fertilization experiment. *Ecology* **99**(11), 2525–2534.
596 **Vicca S., Serrano-Ortiz P., De Boeck H.J., Lemmens C.M.H.M., Nijs I., Ceulemans**
597 **R., … & Janssens I.A. (2007).** Effects of climate warming and declining species richness in
598 grassland model ecosystems: acclimation of CO_2 fluxes. *Biogeosciences* **4**, 27-36.
599 **Vicca S., Luyssaert S., Peñuelas J., Campioli M., Chapin F.S., Ciais P., … &**
600 **Janssens I.A. (2012).** Fertile forests produce biomass more efficiently. *Ecology Letters* **15**,
601 520-526.
602 **Vicca S., Stocker B., Reed S., Wieder W.R., Bahn M., Fay P., … & Ciais P. (2018).**
603 Using research networks to create the comprehensive datasets needed to assess nutrient
604 availability as a key determinant of terrestrial carbon cycling. *Environmental Research Letters*
605 **13**. doi: 10.1088/1748-9326/aaeae7

606 **Vierheilig H., Schweiger P., Brundrett M. (2005).** An overview of methods for the
607 detection and observation of arbuscular mycorrhizal fungi in roots. *Physiologia Plantarum*
608 125, 393-404.
609 **Walinga I., van Vark W., Houba V.J.G. & van der Lee J.J. (1989)** Soil and Plant
610 Analysis, Part 7. In: *Plant analysis procedures*. Agricultural University, Wageningen, 13–16.

TABLES

Table 1: Mean and standard error (SE) of total gross primary production ($\sum GPP$), total rhizosphere respiration ($\sum R_{rhizo}$), total aboveground respiration ($\sum R_{above}$), total autotrophic respiration ($\sum R_{aut}$), belowground plant biomass production (BP_{root}), aboveground plant biomass production (BP_{above}), plant biomass production (BP_{tot}), and the difference between plant C input ($\sum GPP$) and plant C output ($\sum R_{aut} + \sum BP_{tot}$) (C budget imbalance), in g C m^{-2}, for each treatment (P1, P2, P3, P4, P1_noAMF and P4_noAMF). p values and correlation coefficient (R^2) from a linear regression indicate the strength of the relationships with P fertilization (kg P ha^{-1}). p values from one-way ANOVA show pasteurization effects for P4_noAMF versus P4. Subscript letters indicate internal differences between P1, P2, P3 and P4 as results from post-hoc analysis of one-way ANOVA; 95% confidence interval (conf. int.) for C budget imbalance was given.

treatment	$\sum GPP$		$\sum R_{rhizo}$		$\sum R_{above}$		$\sum R_{aut}$		BP_{root}		BP_{above}		BP_{tot}		*C budget imbalance*		
	g C m^{-2}		*g C m^{-2}*		*g C m^{-2}*		*g C m^{-2}*		*g C m^{-2}*		*g C m^{-2}*		*g C m^{-2}*		*g C m^{-2}*		
	mean	*se*	*mean*	*se*	*mean*	*se*	*mean*	*se*	*mean*	*se*	*mean*	*se*	*mean*	*se*	*mean*	*se*	*95% conf. int.*
P1	101.42[a]	5.76	11.21[a]	1.64	41.53[a]	6.51	52.74[a]	6.71	10.60[a]	1.92	37.69[a]	3.83	48.29[a]	4.53	0.39[a]	9.83	-18.88 ~ 19.66
P2	116.86[a]	5.57	15.53[a]	2.32	50.46[a]	6.58	65.99[a]	6.98	14.07[ab]	1.28	41.05[a]	1.33	55.11[a]	2.23	-4.25[a]	9.12	-22.13 ~ 13.63
P3	435.37[b]	6.93	46.34[b]	6.64	219.63[b]	7.60	265.97[b]	10.09	20.87[bc]	3.43	148.20[b]	9.66	169.07[b]	11.52	0.34[a]	15.97	-30.96 ~ 31.64
P4	497.70[b]	7.48	67.15[c]	7.29	257.05[c]	7.22	324.20[c]	10.26	23.25[c]	2.31	179.15[c]	6.46	202.40[c]	7.67	-28.89[a]	14.43	-0.61 ~ -57.17***
P1_noAMF	10.51	NA**	3.21	0.32	5.55	NA**	8.76	NA**	0.20	0.03	1.82	0.15	2.02	0.17	-0.27	NA**	NA**
P4_noAMF	256.10	9.69	15.02	1.37	162.61	8.88	177.62	8.98	13.12	1.06	79.78	7.39	92.90	7.50	-14.43	15.17	-44.16 ~ 15.30
Fertilization effect	p = 0.07		p = 0.03		*p = 0.06		*p = 0.06		*p = 0.01 R^2 = 0.98		p = 0.06 R^2 = 0.92		*p = 0.09 R^2 = 0.95		p = 0.10 R^2 = 0.89		
Pasteurization effect	p = 0.03		p < 0.01		p < 0.01		p < 0.01		p < 0.01		p < 0.01		p < 0.01		p = 0.49		

621 *Notes:* * *significance after ln-transformation; **Data for P1_noAMF were not included in statistical analyses or partitioning calculations, since*

622 *plants were too small for CO_2 measurements and died off prematurely; ***95% conf. int. indicates mean is significantly different from zero*

Table 2: Mean and standard error (SE) of total rhizosphere respiration ($\sum R_{rhizo}$), total aboveground respiration (R_{above}), belowground plant biomass production (BP_{root}), and aboveground plant biomass production (BP_{above}) relative to gross primary production (GPP), the difference between $\sum GPP$ and $\sum R_{aut} + \sum BP_{tot}$ relative to $\sum GPP$ (relative C budget imbalance), and leaf level dark respiration relative to maximum leaf CO_2 assimilation ($R_{dark}:A_{max}$) for each treatment (P1, P2, P3, P4 and P4_noAMF). p values and correlation coefficient (R^2) from a linear regression indicate the strength of the relationships with P fertilization (kg P ha^{-1}). p values from a one-way ANOVA show pasteurization effects for P4_noAMF versus P4. Subscript letters indicate internal differences between P1, P2, P3 and P4 as results from post-hoc analysis of one-way ANOVA.

treatment	$\sum R_{rhizo}:\sum GPP$		$\sum R_{above}:\sum GPP$		$R_{dark} : A_{max}$		$BP_{root}:\sum GPP$		$BP_{above}:\sum GPP$		*relative C budget imbalance*	
	mean	*SE*	*mean*	*SE*	*mean*	*SE*	*mean*	*SE*	*mean*	*SE*	*mean*	*SE*
P1	0.11^{a}	0.02	0.41^{a}	0.07	0.0640^{a}	0.0051	0.10^{a}	0.02	0.37^{a}	0.04	$< 0.01^{a}$	0.10
P2	0.13^{a}	0.02	0.43^{ab}	0.06	0.0685^{ab}	0.0103	0.12^{a}	0.01	0.35^{a}	0.02	-0.04^{a}	-0.08
P3	0.11^{a}	0.02	0.50^{bc}	0.02	0.0931^{b}	0.0082	0.05^{b}	0.01	0.34^{a}	0.02	$< 0.01^{a}$	0.04
P4	0.13^{a}	0.01	0.52^{c}	0.02	0.0892^{b}	0.0071	0.05^{b}	0.005	0.36^{a}	0.01	-0.06^{a}	-0.03
P4_noAMF	0.06	0.01	0.63	0.04	0.0767	0.0078	0.05	0.005	0.31	0.03	-0.06	-0.06
Fertilization effect	p = 0.48		*p = 0.06		p = 0.05 $R^2 = 0.95$		*p = 0.15 $R^2 = 0.83$		p = 0.87 $R^2 = -0.18$		p = 0.23	
Pasteurization effect	p < 0.01		p = 0.01		p = 0.95		p = 0.49		p = 0.16		p = 0.98	

*Note: * significance after ln-transformation*

637 *Table 3:* *Mean and standard error (SE) of mycorrhizal colonization in roots, expressed as %*
638 *of roots colonized by hyphae, arbuscules or vesicules for each treatment (P1, P2, P3, P4,*
639 *P1_noAMF and P4_noAMF). p values and correlation coefficient (R^2) from a linear regression*
640 *indicate the strength of the relationships with P fertilization (kg P ha^{-1}). Subscript letters*
641 *indicate internal differences between P1, P2, P3 and P4 as results from post-hoc analysis of*
642 *one-way ANOVA.*

643

treatment	*mycorrhizal colonization in roots*					
	hyphae		*arbuscules*		*vesicles*	
	%		*%*		*%*	
	mean	*se*	*mean*	*se*	*mean*	*se*
P1	50.40[a]	6.62	11.60[a]	3.12	20.00[a]	6.23
P2	35.60[a]	11.07	7.20[a]	3.72	11.60[a]	5.53
P3	53.20[a]	5.24	9.20[a]	2.42	14.00[a]	2.19
P4	63.73[a]	9.03	22.13[a]	5.81	28.47[a]	6.98
P1_noAMF	0.00	0.00	0.00	0.00	0.00	0.00
P4_noAMF	0.00	0.00	0.00	0.00	0.00	0.00
Fertilization effect	p = 0.08 R^2 = 0.40		p = 0.03 R^2 = 0.50		p = 0.13 R^2 = 0.35	

644

645

646 **FIGURES**

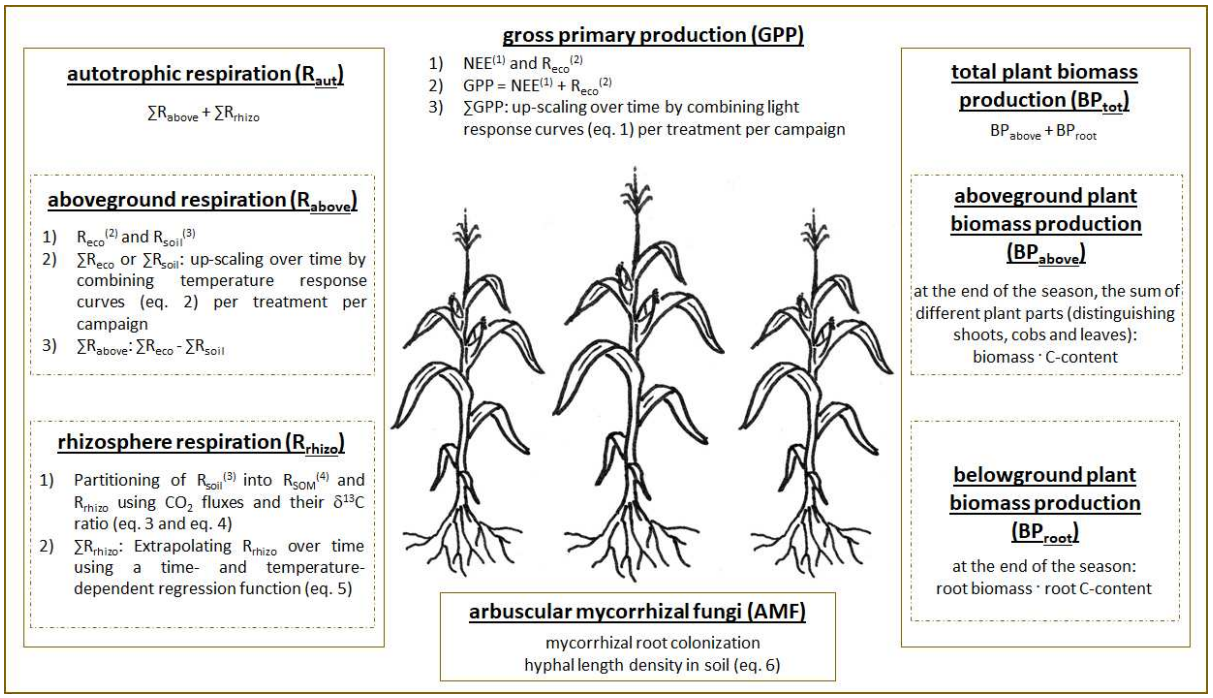

647

648 *Figure 1: overview of the components of plant C partitioning as assessed in the experiment.*

649 *Equations (eq. 1 to 6) refer to the calculations explained in the text (see 'Measurements').*

650 *Notes: NEE(1): net ecosystem exchange of CO_2, estimated from mesocosm-scale measurements*

651 *at various light intensities; R_{eco}(2): total ecosystem CO_2 efflux obtained by measurements in a*

652 *fully darkened chamber; R_{soil}(3): soil respiration obtained by measurements on the shallow soil*

653 *collar; R_{SOM}(4): soil organic matter decomposition CO_2 efflux obtained by measurements on*

654 *the mesocosm-deep collar (i.e., no ingrowth of roots or AMF).*

655

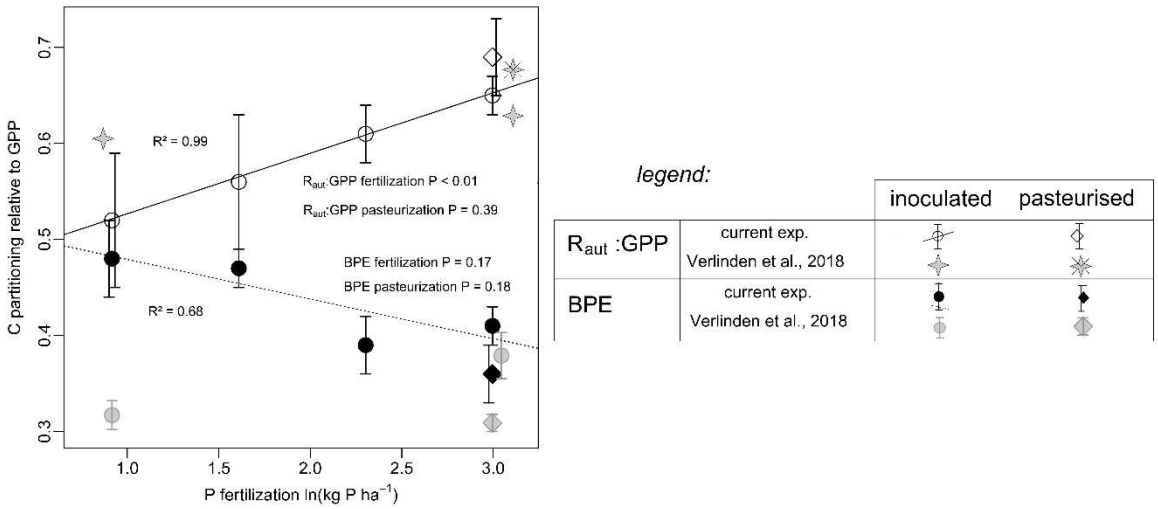

656

657 *Figure 2: Average biomass production efficiency (BPE = total biomass production relative to*
658 *photosynthesis (∑GPP) black), and $\sum R_{aut}$:∑GPP (total autotrophic respiration relative to*
659 *∑GPP, white) for each treatment (P fertilization 2.5, 5, 10 or 20 kg P ha^{-1}) in AMF inoculated*
660 *mesocosms (o) and pasteurized P4 mesocosms (P4_noAMF, ◊). p values are shown for a linear*
661 *regression between BPE or $\sum R_{aut}$:∑GPP versus P fertilization (kg P ha^{-1}). A full line indicates*
662 *statistical significant, a dotted line indicates that the regression was not statistically*
663 *significant. p values for the pasteurization effect are obtained from a one-way ANOVA*
664 *comparing P4_noAMF to P4. Error bars show +/- 1 standard error (SE). BPE and*
665 *$\sum R_{aut}$:∑GPP of comparable treatments from Verlinden et al. (2018) are also shown (grey*
666 *circles and grey stars, respectively).*

667

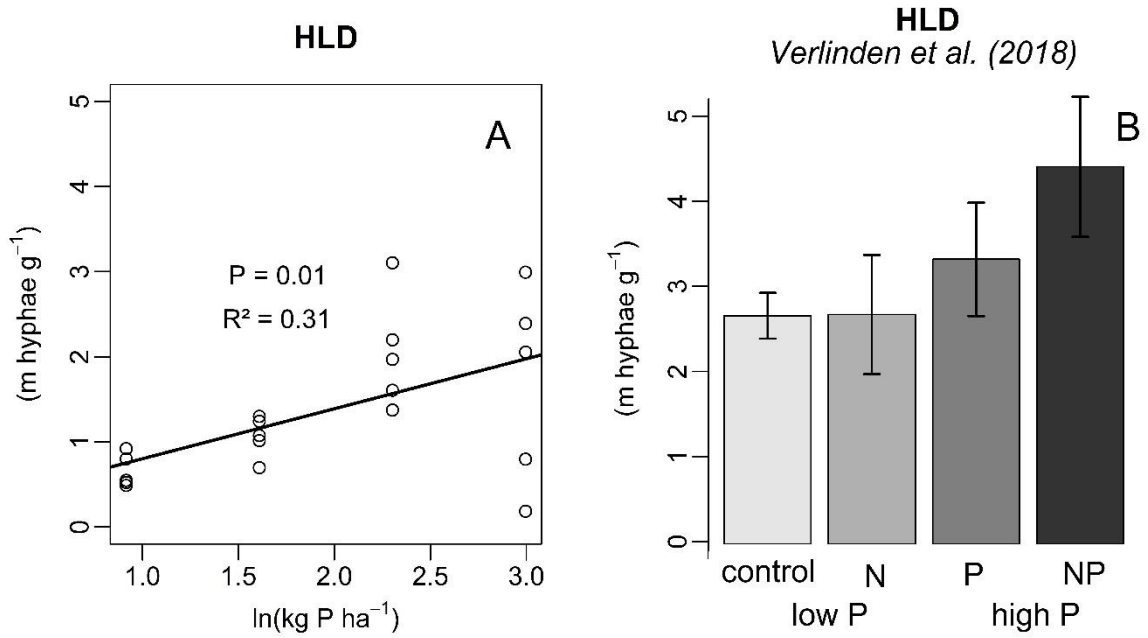

668

669 *Figure 3: hyphal length density (HLD; m hyphae g^{-1} sand) in mesh bags for each treatment (P*
670 *fertilization; log(kg P ha^{-1})) in AMF inoculated mesocosms (A). p values and correlation*
671 *coefficient (R^2) from a linear regression indicate the strength of the relationships with P*
672 *fertilization (kg P ha^{-1}) after ln-transformation. Average and SE of HLD from Verlinden et al.*
673 *(2018) are shown in panel (B).*

SUPPORTING INFORMATION LEGENDS

Appendix S1: experimental set up and soil mixture, as in Verlinden et al. (2018).

Appendix S2: CO_2 fluxes data analyses for mean seasonal values and standard errors (SE) for GPP, R_{eco} and R_{soil}.

Appendix S3: the use of T_{soil} instead of T_{air} for calculating and upscaling R_{eco}.

Appendix S4: Rhizosphere respiration (R_{rhizo}) calculations and estimation of total R_{rhizo} ($\sum R_{rhizo}$) over the entire growing season, as in Ven et al. (2019).

Appendix S5: Hyphal extraction from mesh bag sand following the approach of Rillig et al. (1999).

Table S1: mean and standard error (SE) of soil organic matter (SOM) % C and $\delta^{13}C$ ratio, and root $\delta^{13}C$ ratio at the start of the previous experiment (Verlinden et al., 2018) and the current experiment.

Table S2: mean, standard error (SE) and correlation coefficient after statistical analysis (r) of cumulated rhizosphere respiration ($\sum R_{rhizo}$) ($\mu mol\ C\ m^{-2}\ s^{-1}$) calculated with and without adding an intercept for day 0, $R_{rhizo} = 0$ to the dataset.

Table S3: mean and standard error (SE) of dark respiration (R_{dark}), maximum leaf CO_2 assimilation (A_{max}) and their ratio (R_{dark}:A_{max}) for each treatment (P1, P2, P3, P4 and P4_noAMF).

699

700 *Table S4: R_{soil} as a percentage of R_{eco} for seven time periods, starting at day of planting (21/06)*
701 *and ending at plant harvest (31/08).*

702

703 *Table S5: R^2 of fits using soil temperature (T_{soil}) or air temperature (T_{air}) to calculate $\sum R_{eco}$,*
704 *and the difference between R^2 of these fits using T_{soil} and T_{air}, for each treatment in four time*
705 *periods during the current experiment. Mean, maximum (max) and minimum (min) R^2 over*
706 *these four time periods for each treatment are given.*

707

708 *Table S6: R^2 of fits using soil temperature (T_{soil}) or air temperature (T_{air}) to calculate $\sum R_{eco}$,*
709 *and the difference between R^2 of these fits using T_{soil} and T_{air}, for each treatment in seven time*
710 *periods during the experiment of Verlinden et al. (2018). Mean, maximum (max) and minimum*
711 *(min) R^2 over these seven time periods for each treatment are given.*

712

713 *Table S7: $\sum R_{eco}$ at the end of the experiment discussed in Verlinden et al. (2018), and their*
714 *difference and deviation (%) for each treatment. The mean deviation was calculated over all*
715 *treatments (in **bold**).*

716

717 *Table S8: Results for using soil temperature (T_{soil}) to calculate and upscale ecosystem*
718 *respiration (R_{eco}). Average (mean) and standard error (SE) of total gross primary production*
719 *($\sum GPP$), total aboveground respiration ($\sum R_{above}$), total autotrophic respiration ($\sum R_{aut}$), the*
720 *difference between plant C input ($\sum GPP$) and plant C output ($\sum R_{aut}$ + BP_{tot} = C budget*
721 *imbalance), in g C m^{-2} and of $\sum R_{above}$, $\sum R_{aut}$ and C budget imbalance relative to gross primary*
722 *production (GPP), i.e. respectively $\sum R_{above}$:$\sum GPP$, $\sum R_{aut}$:$\sum GPP$ and the relative C budget*

723 *imbalance for each treatment (P1, P2, P3, P4 and P4_noAMF). These results and their*
724 *statistics can also be found in Tables 1, 2 and Fig. 2.*
725
726 *Table S9: Results for using air temperature (T_{air}) to calculate and upscale ecosystem*
727 *respiration (R_{eco}). Average (mean) and standard error (SE) of total gross primary production*
728 *($\sum GPP$), total aboveground respiration ($\sum R_{above}$), total autotrophic respiration ($\sum R_{aut}$), the*
729 *difference between plant C input ($\sum GPP$) and plant C output ($\sum R_{aut} + BP_{tot}$ = C budget*
730 *imbalance), in g C m^{-2} and of $\sum R_{above}$, $\sum R_{aut}$ and C budget imbalance relative to gross primary*
731 *production (GPP), i.e. respectively $\sum R_{above}$:$\sum GPP$, $\sum R_{aut}$:$\sum GPP$ and the relative C budget*
732 *imbalance for each treatment (P1, P2, P3, P4 and P4_noAMF).*
733
734 *Table S10: mean, standard error (SE) and correlation coefficient after statistical analysis (R^2)*
735 *of cumulated rhizosphere respiration ($\sum R_{rhizo}$) (μmol C m^{-2} s^{-1}) relative to belowground plant*
736 *biomass production (BP_{root}) and aboveground plant biomass production (BP_{above}). p values*
737 *from a linear regression show correlations with P fertilization; p values from one-way ANOVA*
738 *show pasteurization effect between P4 and P4_noAMF.*
739 *Note: * significance after ln-transforming*
740
741 *Table S11: mean and standard error (between brackets) pH at the start, the middle and the end*
742 *of the previous experiment (2016; published in Verlinden et al., 2018) and the current*
743 *experiment (2017).*
744
745 *Table S12: mean and standard error (SE) of P and N concentration ([P] and [N]), and its N:P*
746 *ratio of leaves in different treatments in 2017 and 2016, for 2017. p value of ANOVA showed*
747 *significance in differences due to fertilization or pasteurization (P4 vs. P4_noAMF).*

748

749 *Figure S1: comparison of CO_2 flux measurement cuvettes.*

750

751 *Figure S2: observed (black circles) and predicted (grey triangles) rhizosphere respiration*
752 *(R_{rhizo}) ($\mu mol\ C\ m^{-2}\ s^{-1}$) in time (days since planting) for each phosphorus (P) fertilization*
753 *treatment. Correlation coefficient (R^2) reflects the goodness of fit for observed vs. predicted.*